

Level Density in the Complex Scaling Method

Ryusuke SUZUKI,¹ Takayuki MYO² and Kiyoshi KATŌ¹

¹*Division of Physics, Graduate School of Science, Hokkaido University,
Sapporo 060-0810, Japan*

²*Research Center for Nuclear Physics (RCNP), Osaka University, Ibaraki
567-0047, Japan*

(Received February 3, 2005)

It is shown that the continuum level density (CLD) at unbound energies can be calculated with the complex scaling method (CSM), in which the energy spectra of bound states, resonances and continuum states are obtained in terms of L^2 basis functions. In this method, the extended completeness relation is applied to the calculation of the Green functions, and the continuum-state part is approximately expressed in terms of discretized complex scaled continuum solutions. The obtained result is compared with the CLD calculated exactly from the scattering phase shift. The discretization in the CSM is shown to give a very good description of continuum states. We discuss how the scattering phase shifts can inversely be calculated from the discretized CLD using a basis function technique in the CSM.

§1. Introduction

Recently, there has been much interest in nuclear structures of unstable nuclei, in which exotic nuclear structures have been revealed through the development of radioactive nuclear beam experiments.¹⁾ It has been shown that for such nuclei, for example the so-called neutron halo nuclei, there are extremely weak binding ground states, and most of the excited states are in the continuum energy region. Therefore, to understand the exotic structures and excitations of these nuclei, it is necessary to study continuum and resonant states in unbound energy regions.

The continuum level density (CLD) is expected to play an important role in relating experimental data and theoretical models for unbound states. Recently, Kruppa and Arai²⁾⁻⁴⁾ proposed an interesting method to calculate the CLD and argued that resonance parameters can be determined from the CLD. They start their investigation from the definition of the CLD,⁵⁾

$$\Delta(E) = -\frac{1}{\pi} \text{Im} [\text{Tr} [G(E) - G_0(E)]], \quad (1.1)$$

where the full and free Green functions are given by $G(E) = (E - H)^{-1}$ and $G_0(E) = (E - H_0)^{-1}$, respectively. Because the Hamiltonian H includes finite range interactions in addition to the asymptotic Hamiltonian H_0 , the CLD expresses the effect from the interactions. When the eigenvalues (ϵ_i and ϵ_0^j , respectively) of H and H_0 are obtained approximately within a framework including a finite number (N)

of basis functions, the following discrete level density is defined:

$$\Delta_N(E) = \sum_i^N \delta(E - \epsilon_i) - \sum_j^N \delta(E - \epsilon_0^j). \quad (1.2)$$

Kruppa²⁾ employed a smoothing technique defined by the Strutinsky procedure⁶⁾ to calculate the continuous CLD, $\Delta(E)$, from its discrete form, $\Delta_N(E)$. However, as discussed in Ref. 4) their results for the CLD exhibit a strong dependence on the smoothing parameters. We desire a more effective method to smooth the discrete quantities, or to discretize the continuum states.

In this paper, we study a more direct method to calculate the CLD with no smoothing technique in the framework of complex scaling,⁷⁾ in which a basis function method is used to obtain not only bound states but also resonance and continuum states. The idea for the present method is taken from the extended completeness relation,⁸⁾ originally proposed by Berggren,⁹⁾ for bound, resonance and continuum states in the complex scaling method (CSM). Exact proofs of this extended completeness relation for the CSM were recently given for a coupled channel system¹⁰⁾ and a single channel system.¹¹⁾ Green functions can be expressed by using the extended completeness relation in terms of discrete eigenvalues of the CSM with a finite number of basis functions. Because the complex scaled Hamiltonians H^θ and H_0^θ have complex eigenvalues, singularities, like the δ -function contained in Eq. (1.2), are avoided and replaced by Lorentzian functions. Therefore, no smoothing process is needed. Furthermore, it is shown that $\Delta(E)$ for the CLD can be calculated independently of the scaling parameters in the CSM.

Kruppa and Arai²⁾⁻⁴⁾ applied the CLD to search for resonance parameters. However, although parameter values for narrow resonances can be obtained using any method of CSM and CLD, it is not easy to extract parameter values for broad resonances with the CLD. Rather than obtaining such resonance parameters, it is more important to calculate the phase shift and/or S-matrix for the scattering states from the CLD. The CLD $\Delta(E)$ is related to the scattering phase shift $\delta(E)$ as^{5),12)}

$$\Delta(E) = \frac{1}{\pi} \frac{d\delta(E)}{dE}. \quad (1.3)$$

Therefore, once we confirm that the CLD calculated in the present method is consistent with $\Delta(E)$ obtained from the phase shift of the scattering solution, we can inversely calculate the phase shift by integrating the CLD obtained as a function of the energy from the eigenvalues of the complex scaled Hamiltonians. This implies that the phase shift can be calculated from discrete eigenvalues using a basis function method.

We here demonstrate the reliability of this method by applying it to several two-body systems, including ${}^4\text{He}+n$ and $\alpha+\alpha$, which were studied by Arai and Kruppa.⁴⁾ Comparing the calculated continuum level density and the phase shifts in the CSM with the results obtained from the exactly calculated phase shifts and their derivatives (the CLD), we show that the extended completeness relation in the CSM is effective, and also that the phase shift is satisfactorily reproduced by the discretized solutions for continuum states.

In §2, we explain the formalism for treating the level density in the complex scaling method. We study the reliability of this method by applying it to a simple potential model in §3, and we investigate ${}^4\text{He}+n$ and $\alpha+\alpha$ systems in §4. In §5, a summary and conclusions are given.

§2. Continuum level density in the complex scaling method

Here we briefly explain the complex scaling method (CSM). In the CSM, the spatial coordinate \mathbf{r} and the wave number \mathbf{k} transform as

$$U(\theta) : \mathbf{r} \rightarrow \mathbf{r} \exp(i\theta), \quad \mathbf{k} \rightarrow \mathbf{k} \exp(-i\theta), \quad (2.1)$$

where $U(\theta)$ is a scaling operator and θ is a real number called a scaling parameter. Under this transformation, the asymptotic divergent behavior, $\sim \exp(ik_r r)$, of a resonant state with a complex wave number $k_r = \kappa - i\gamma$ is changed into a damping form, $\exp\{i(\kappa - i\gamma)(r \cos \theta + ir \sin \theta)\} = \exp\{(\gamma \cos \theta - \kappa \sin \theta)r\} \cdot \exp\{i(\kappa \cos \theta + \gamma \sin \theta)r\}$ for $\theta > \tan^{-1} \gamma/\kappa$. Therefore, resonant states and bound states are obtained as discrete solutions of the complex scaled Schrödinger equation

$$H(\theta)\Phi^\theta = E\Phi^\theta, \quad (2.2)$$

where $H(\theta) = U(\theta)HU^{-1}(\theta)$. Because we require the complex scaled Hamiltonian to have no singularity, the scaling parameter θ has an upper limit, θ_C . For the Gaussian potential, $\theta_C = \pi/4$. For $\theta < \theta_C$, the solutions of bound states and resonances with $\gamma/\kappa < \tan \theta$ are square-integrable, because of their damping forms in the asymptotic region. Therefore, employing an appropriate scaling parameter θ , we can derive resonant states in addition to bound states using a square-integrable basis expansion, for example, in terms of harmonic oscillator or Gaussian functions $\{\phi_n\}$:

$$\Phi^\theta = \sum_{n=1}^N c_n(\theta)\phi_n. \quad (2.3)$$

In Fig. 1, we present a schematic eigenvalue distribution for the complex scaled Schrödinger equation. It is seen that the energies of bound states are not changed from the spectral positions of the original Hamiltonian. The eigenvalues of the resonant states, which are particularly noteworthy, are obtained as $E = E_r - i\Gamma_r/2$, where E_r and Γ_r are the energy and width of a resonance, respectively. By contrast, the continuum spectra of the Hamiltonian $H(\theta)$ are distributed on the 2θ -lines originating from every threshold. If we do not apply the complex scaling, the original Schrödinger equation gives the continuum spectra, including resonances on the positive energy axis. Under complex scaling, the resonances for which $\gamma/\kappa < \tan \theta$ are separated from the continuum, and the rotated continuum spectra starting from different threshold energies are separately obtained on different 2θ -lines. Furthermore, when we apply a basis function method to solve the complex scaled Schrödinger equation, these continuum spectra are discretized on different 2θ -lines, as shown in Fig. 1.

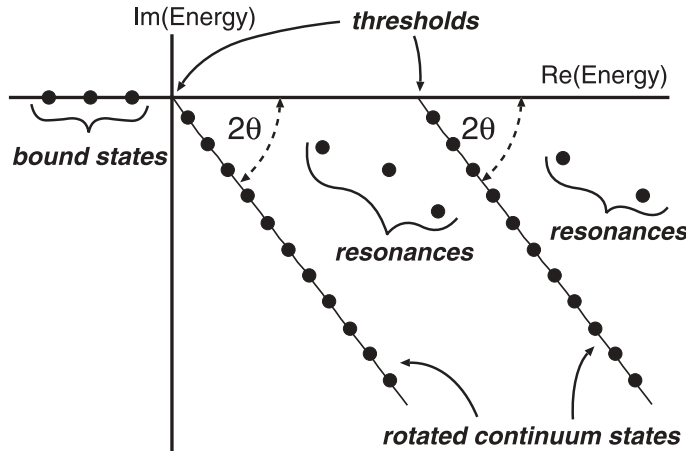


Fig. 1. Schematic energy eigenvalue distribution for a complex scaled Hamiltonian.

Let us return to the problem of the level density. The level density $\rho(E)$ of the Hamiltonian H is defined as

$$\rho(E) = \sum \delta(E - E_i), \tag{2.4}$$

where the quantities E_i are the eigenvalues of H , and the summation and integration are taken for discrete and continuous eigenvalues, respectively. This definition of the level density can also be expressed using the Green function:

$$\begin{aligned} \rho(E) &= -\frac{1}{\pi} \text{Im} \left\{ \text{Tr} \left[\frac{1}{E - H} \right] \right\} \\ &= -\frac{1}{\pi} \text{Im} \int d\mathbf{r} \left\langle \mathbf{r} \left| \frac{1}{E - H} \right| \mathbf{r} \right\rangle. \end{aligned} \tag{2.5}$$

Here, applying the CSM and the extended completeness relation (ECR)^{8),9)} to the expression of the Green function, we obtain

$$\begin{aligned} \rho(E) &= -\frac{1}{\pi} \text{Im} \int d\mathbf{r} \left\langle \mathbf{r} \left| U(\theta)^{-1} U(\theta) \frac{1}{E - H} U(\theta)^{-1} U(\theta) \right| \mathbf{r} \right\rangle \\ &= -\frac{1}{\pi} \text{Im} \int d\mathbf{r} \left\langle \mathbf{r}_\theta \left| \frac{1}{E - H(\theta)} \right| \mathbf{r}_\theta \right\rangle \\ &= -\frac{1}{\pi} \text{Im} \int d\mathbf{r} \left[\sum_B^{N_B} \frac{\Phi_B^\theta(\mathbf{r}) \tilde{\Phi}_B^{\theta*}(\mathbf{r})}{E - E_B} + \sum_R^{N_R^\theta} \frac{\Phi_R^\theta(\mathbf{r}) \tilde{\Phi}_R^{\theta*}(\mathbf{r})}{E - E_R} + \int_{L_\theta} dk_\theta \frac{\Phi_{k_\theta}^\theta(\mathbf{r}) \tilde{\Phi}_{k_\theta}^{\theta*}(\mathbf{r})}{E - E_{k_\theta}} \right], \end{aligned} \tag{2.6}$$

where N_B and N_R^θ are the numbers of bound states and resonances in the wedge region between the real energy axis and the 2θ -lines, respectively. A detailed explanation of the extended completeness relation is given in Ref. 8).

In the integration over \mathbf{r} in Eq. (2.6), the bound state and resonance parts are easily found to be unity, because of the normalization of the wave functions, but the continuum part cannot be calculated, due to the singular nature of the integration. This singularity is eliminated when we discretize the continuum spectra using the basis function method with a finite number N of basis functions. Then, the approximate density of states $\rho_\theta^N(E)$ for the basis number N is expressed as

$$\rho_\theta^N(E) = \sum_B^{N_B} \delta(E - E_B) - \frac{1}{\pi} \text{Im} \sum_R^{N_R^\theta} \frac{1}{E - E_R} - \frac{1}{\pi} \text{Im} \sum_k^{N - N_B - N_R^\theta} \frac{1}{E - \mathcal{E}_k(\theta)}. \tag{2.7}$$

As explained above, the energy of the resonance is obtained as $E_R = E_r - i\Gamma_r/2$, and thus each resonance term has the Breit-Wigner form

$$\text{Im} \frac{1}{E - E_R} = \frac{-\Gamma_r/2}{(E - E_r)^2 + \Gamma_r^2/4}. \tag{2.8}$$

For the continuum part, discretized continuum states are obtained on the 2θ -line in the complex energy plane, $\mathcal{E}_k(\theta) = \mathcal{E}_k^R - i\mathcal{E}_k^I$, where $\mathcal{E}_k^I/\mathcal{E}_k^R = \tan 2\theta$. Therefore, the continuum part in the level density can be expressed in terms of a Lorentzian function whose form is similar to the Breit-Wigner form:

$$\text{Im} \frac{1}{E - \mathcal{E}_k(\theta)} = \frac{-\mathcal{E}_k^I}{(E - \mathcal{E}_k^R)^2 + \mathcal{E}_k^I^2}. \tag{2.9}$$

Inserting Eqs. (2.8) and (2.9) into Eq. (2.7), we obtain the level density in the basis function method as

$$\rho_\theta^N(E) = \sum_B^{N_B} \delta(E - E_B) + \frac{1}{\pi} \sum_R^{N_R^\theta} \frac{\Gamma_r/2}{(E - E_r)^2 + \Gamma_r^2/4} + \frac{1}{\pi} \sum_k^{N - N_B - N_R^\theta} \frac{\mathcal{E}_k^I}{(E - \mathcal{E}_k^R)^2 + \mathcal{E}_k^I^2}. \tag{2.10}$$

Here, it is noted that $\rho_\theta^N(E)$ has a θ dependence, but $\rho(E)$ does not. This θ dependence problem of $\rho_\theta^N(E)$ is due to the fact that we employ a finite number of basis functions, and it can be solved by introducing $\Delta(E)$ defined in Eq. (1.1). The continuum level density (CLD) $\Delta(E)$ is expressed as a balance between the density of states $\rho(E)$ obtained from the Hamiltonian H and the density of continuum states, $\rho_0(E)$, obtained from the asymptotic Hamiltonian H_0 in the form

$$\Delta(E) = \bar{\rho}(E) - \rho_0(E), \tag{2.11}$$

where $\bar{\rho}(E)$ is defined through subtraction of the bound state term from $\rho(E)$. Physically, $\Delta(E)$ represents the density of unbound levels, which result from the interaction with a finite range. This can also be understood from the fact that $\Delta(E)$ is related to the phase shift caused by the interaction.

In the basis function method with a finite number N of basis states, we have

$$\Delta_{\theta}^N(E) = \bar{\rho}_{\theta}^N(E) - \rho_{0(\theta)}^N(E). \quad (2.12)$$

The first term on the right-hand side represents the level density in which the bound state term is subtracted from Eq. (2.7), and the second term is expressed in terms of the eigenvalues $\mathcal{E}_k^0(\theta) = \mathcal{E}_k^{0R} - i\mathcal{E}_k^{0I}$ of the asymptotic Hamiltonian $H_0(\theta)$, which has only continuum spectra on the 2θ -lines:

$$\rho_{0(\theta)}^N(E) = \frac{1}{\pi} \sum_k^N \frac{\mathcal{E}_k^{0I}}{(E - \mathcal{E}_k^{0R})^2 + \mathcal{E}_k^{0I^2}}. \quad (2.13)$$

Thus, we have

$$\begin{aligned} \pi \Delta_{\theta}^N(E) = & \sum_R^{N_R^{\theta}} \frac{\Gamma_r/2}{(E - E_r)^2 + \Gamma_r^2/4} + \sum_k^{N - N_B - N_R^{\theta}} \frac{\mathcal{E}_k^I}{(E - \mathcal{E}_k^R)^2 + \mathcal{E}_k^{I^2}} \\ & - \sum_k^N \frac{\mathcal{E}_k^{0I}}{(E - \mathcal{E}_k^{0R})^2 + \mathcal{E}_k^{0I^2}}. \end{aligned} \quad (2.14)$$

As shown by the numerical results presented in the next section, the θ dependence of $\Delta_{\theta}^N(E)$ disappears through the cancellation of the θ dependence in the second and third terms of Eq. (2.14). When we consider a small value of θ , and therefore no resonance exists in the wedge region, the CLD can be expressed in terms of only the second and third terms.

§3. Simple potential model

We now examine the reliability of the present method for a simple potential model. As a schematic potential, we employ the CGKPM potential,¹³⁾ whose resonance structure has been studied in detail. The Hamiltonian in this case is given by

$$H = T + V, \quad T = -\frac{\hbar^2}{2\mu} \nabla^2, \quad V(r) = -8.0e^{-0.16r^2} + 4.0e^{-0.04r^2}, \quad (3.1)$$

where we set $\hbar^2/\mu = 1$ (MeV/fm²) for simplicity. The Schrödinger equation for this Hamiltonian is solved by applying the basis function method, and thus we write

$$\psi(\mathbf{r}) = \sum_{lm} R_{\ell}(r) Y_{\ell m}(\hat{r}), \quad R_{\ell}(r) = \sum_i^N c_i^{\ell} \phi_{\ell}(r, b_i). \quad (3.2)$$

For each partial wave, we use Gaussian functions¹⁴⁾ with different size parameters as basis functions:

$$\phi_{\ell}(r, b_i) = N_{\ell}(b_i) \cdot r^{\ell} \exp\left[-\frac{1}{2b_i^2} r^2\right], \quad N_{\ell}(b_i) = b_i^{-3/2-\ell} \left\{ \frac{2^{\ell+2}}{(2\ell+1)!!\sqrt{\pi}} \right\}^{1/2}, \quad (3.3)$$

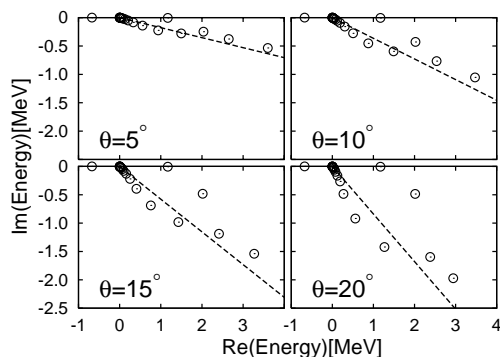


Fig. 2. Energy eigenvalue distribution of the 1^- states for the complex scaled Hamiltonian of the simple potential model given by Eq. (3.1). The circles represent eigenvalues and dashed lines are 2θ -lines.

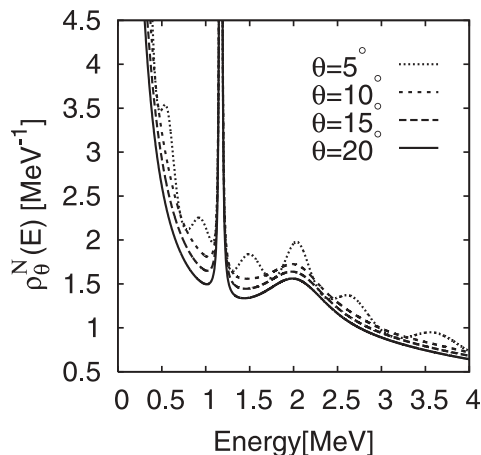


Fig. 3. The level density $\rho_{\theta}^N(E)$ calculated for different values of θ .

where the parameters $\{b_i : i = 1, 2, \dots, N\}$ are given by a geometrical progression¹⁴⁾ of the form

$$b_i = b_0 \gamma^{i-1}. \tag{3.4}$$

Here, b_0 and γ are the first term and the common ratio, respectively. We employ $N = 30$, $b_0 = 0.2$ fm and $\gamma = 1.2$ in the following calculations. Of course, the same results are obtained even if other kinds of basis functions (for example, harmonic oscillator functions) are used.

In Fig. 2, we plot the energy eigenvalue distribution of the 1^- states. One bound state (-0.67 MeV) and many resonant states exist: The three lowest resonances are $1.1710 - i0.0049$ (MeV), $2.0175 - i0.4863$ (MeV) and $2.5588 - i1.7378$ (MeV).¹⁵⁾ The lowest resonance is obtained with the CSM for $\theta = 5^\circ$, but the second lowest resonance is not obtained for this scaling parameter value. The second resonance appears clearly when $\theta > 10^\circ$. The continuum solutions vary slightly from the 2θ -line, and the dispersion increases for large values of θ . However, this distribution of continuum eigenvalues depends on the choice of the basis functions, and it creates no difficulty in the CLD calculations.

Using these eigenvalues, we calculate the level density $\rho_{\theta}^N(E)$ given by Eq. (2.7), and we display the result in Fig. 3. Oscillatory behavior is seen at $\theta = 5^\circ$, but this oscillation is smoothed when θ is larger than 10° . Even at $\theta = 5^\circ$, the oscillation may disappear if we employ a large number of basis functions so that the intervals between the discretized continuum eigenvalues become smaller than their imaginary parts. However, it is easier to choose a larger value of θ in order to increase the imaginary parts of the discretized continuum eigenvalues. The intervals between the discretized continuum eigenvalues depend on the number N of basis functions. The critical value of θ may be defined as the scaling angle at which the imaginary parts of the discretized continuum eigenvalues become larger than the intervals between the eigenvalues. This critical value of θ depends on N , and therefore we express it

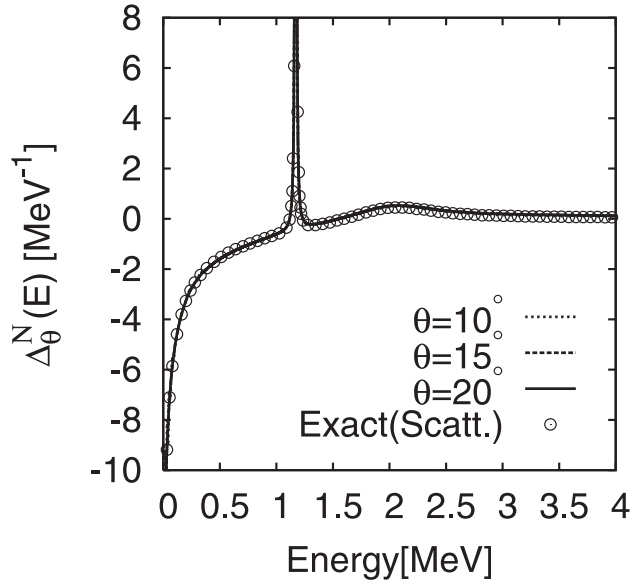


Fig. 4. The complex scaled CLD $\Delta_{\theta}^N(E)$ for $\theta = 10^\circ$, 15° and 20° and the exact solution obtained by solving the scattering problem.

as θ_N . When θ becomes larger than 10° in the present simple potential case, $\rho_{\theta}^N(E)$ exhibits the same behavior, and therefore we can set $\theta_N \approx 10^\circ$. For $\theta > \theta_N$, only the absolute values of $\rho_{\theta}^N(E)$ depend on θ .

This θ dependence of the absolute values of $\rho_{\theta}^N(E)$ can be canceled through subtraction of $\rho_{0\theta}^N(E)$; that is, we show that the CLD $\Delta_{\theta}^N(E)$ defined in Eq. (2.14) has no θ dependence for $\theta \geq \theta_N$. In Fig. 4, we plot the CLD $\Delta_{\theta}^N(E)$ calculated for $\theta = 10^\circ$, 15° and 20° and compare it with the result of the exact calculation. Here, “exact” means that we calculate the CLD $\Delta(E)$ from the phase shift using Eq. (1.3). The phase shift is obtained with the help of the scattering solution without any approximation. From Fig. 4, we see that it is quite difficult to distinguish the plots of $\Delta_{\theta}^N(E)$ calculated for $\theta = 10^\circ$, 15° and 20° . They are all consistent with the exact calculation. This result indicates that the CLD $\Delta(E)$ can be approximated by $\Delta_{\theta}^N(E)$ in the CSM, and the phase shift can be obtained from $\Delta_{\theta}^N(E)$ without solving the scattering problem.

§4. Applications to ${}^4\text{He}+n$ and $\alpha + \alpha$ systems

We now apply the present method to realistic two-body systems of ${}^4\text{He}+n$ and $\alpha + \alpha$. The ${}^4\text{He}+n$ system has rather broad resonances but no bound state, and the $\alpha + \alpha$ system also has no bound state but a sharp resonance due to the Coulomb barrier. The Coulomb potential is a typical long-range potential and is represented by the asymptotic term of H_0 . The antisymmetrization among clusters in both the systems ${}^4\text{He}+n$ and $\alpha + \alpha$ is carried out with the orthogonality condition model (OCM).¹⁶⁾ We show that the present method is very useful in analyses of continuum

states of such realistic cluster systems.

4.1. ${}^4\text{He}+n$ system

The wave function of ${}^5\text{He}$ with spin J is expressed in the ${}^4\text{He}+n$ cluster model as

$$\Phi^J({}^5\text{He}) = \mathcal{A} \{ \Phi({}^4\text{He}) \cdot \psi_{\text{rel}}^J(\mathbf{r}) \}, \quad (4.1)$$

where \mathcal{A} , $\Phi({}^4\text{He})$ and $\psi_{\text{rel}}^J(\mathbf{r})$ are the antisymmetrizer, the internal wave function of ${}^4\text{He}$ assuming a $(0s_{1/2})^4$ configuration, and the relative wave function between ${}^4\text{He}$ and the valence neutron, respectively. We solve the relative wave function $\psi_{\text{rel}}^J(\mathbf{r})$ by applying the OCM. This yields

$$[T_{\text{rel}} + V_{\text{cn}}(r) + \lambda |\phi_{\text{PF}}\rangle\langle\phi_{\text{PF}}| - E] \psi_{\text{rel}}^J(\mathbf{r}) = 0, \quad (4.2)$$

where T_{rel} and $V_{\text{cn}}(r)$ are the kinetic energy and potential operators for the ${}^4\text{He}-n$ relative motion, respectively. In this calculation, we use the so-called KKNN potential¹⁷⁾ for $V_{\text{cn}}(r)$, which provides an accurate description of the low-energy scattering data for this system. The third term, constituting the non-local potential in Eq. (4.2) represents the projection operator to remove the Pauli forbidden (PF) states [which is the $(0s_{1/2})$ state in this case] from the relative motion,¹⁸⁾ and λ is taken as 10^6 MeV in this calculation.

Equation (4.2) is solved by using the basis functions, as explained in the previous section, and we obtain

$$\psi_{\text{rel}}^J(\mathbf{r}) = [Y_\ell(\hat{r})\chi_{1/2}]_J \varphi_\ell(r), \quad \varphi_\ell(r) = \sum_i^N c_i^\ell \phi_\ell(r, b_i), \quad (4.3)$$

where $[Y_\ell(\hat{r})\chi_{1/2}]_J$ is a function of the orbital angular momentum and spin coupled to J , and the radial wave function $\varphi_\ell(r)$ is expanded in the Gaussian basis functions $\{\phi_\ell(r, b_i)\}$, which are defined in Eq. (3.3).

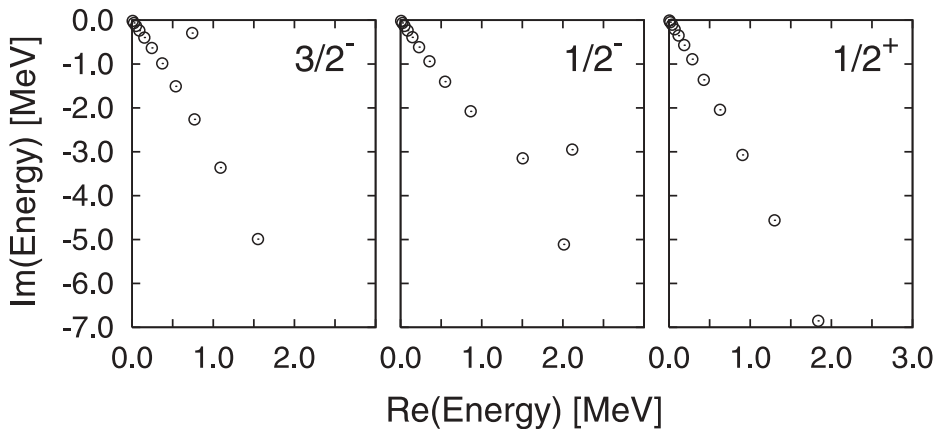


Fig. 5. Energy eigenvalue distributions of the ${}^4\text{He}-n$ system for the $J^\pi = 3/2^-, 1/2^-$ and $1/2^+$ states, where θ is taken as 35° .

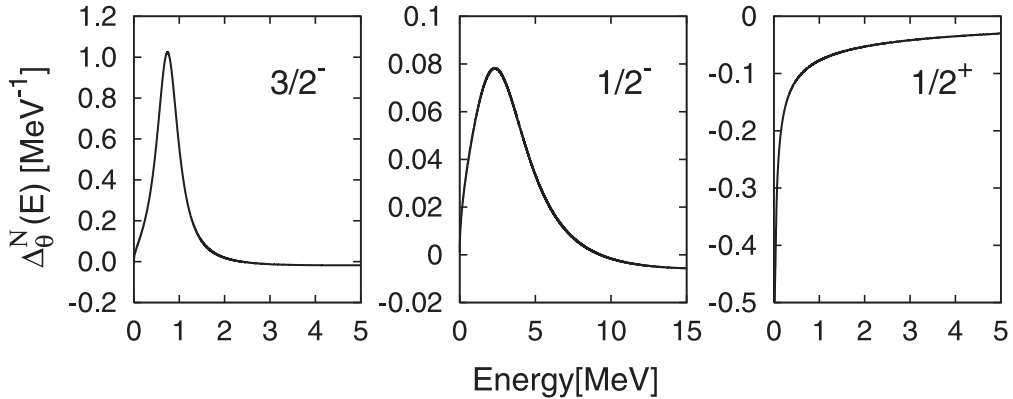


Fig. 6. Continuum level densities of the ${}^4\text{He}\text{-}n$ system for the $J^\pi = 3/2^-, 1/2^-$ and $1/2^+$ states.

Using the same basis set as in the case of the simple model, we calculate the energy eigenvalues of the complex scaled Hamiltonian with $\theta = 35^\circ$, and the results for the three states $3/2^-$, $1/2^-$ and $1/2^+$ are shown in Fig. 5. We can see that each of the states $3/2^-$ and $1/2^-$ has one resonance pole, corresponding to the observed resonances of ${}^5\text{He}$. The $1/2^+$ state has no resonance. Resonant structures of ${}^5\text{He}$ have been investigated in detail with the complex scaling method by Aoyama et al.¹⁹⁾ In addition to resonances, the discretized continuum solutions have been obtained along the 2θ -line. Several continuum solutions are off the 2θ -line. It is believed that the reason for this is that the couplings between the continuum and resonance are not correctly described because the number of basis functions is not large enough. However, the resonant solutions are obtained with appropriate accuracy, and the CLD is obtained from these continuum solutions satisfactorily, although the positions

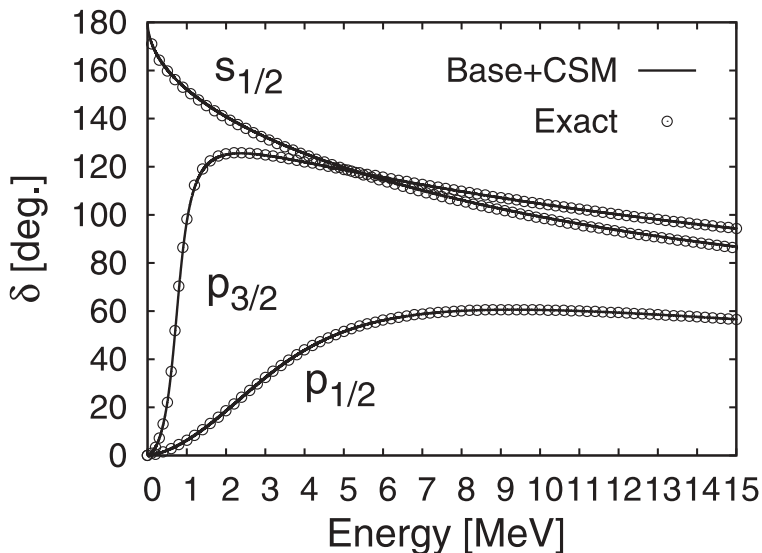


Fig. 7. Scattering phase shifts of the ${}^4\text{He}\text{-}n$ system for the $J^\pi = 3/2^-, 1/2^-$ and $1/2^+$ states.

of some continuum solutions are slightly off the 2θ -line.

Applying Eq. (2.14) to the obtained eigenvalue distribution of the complex scaled Hamiltonian for the $3/2^-$, $1/2^-$ and $1/2^+$ states, we calculate the CLD of the ${}^4\text{He}$ - n system. The results are shown in Fig. 6. It is seen that each of the $3/2^-$ and $1/2^-$ states has a peak, but the $1/2^+$ state has no peak. The position and width of the peaks in the CLD for the $3/2^-$ and $1/2^-$ states correspond to their resonance energy and width. These results are very similar to those for the CLD distributions calculated by Arai and Kruppa,⁴⁾ except for the absolute strengths. In the calculation of the CLD carried out by Arai and Kruppa, the result depends on the smoothing parameter.

To see the reliability of the CLD obtained here, we calculate the phase shift from the obtained CLD. In Fig. 7, we show the scattering phase shifts of the $3/2^-$, $1/2^-$ and $1/2^+$ states. We compare these results with the exact phase shifts, and we find very good quantitative agreement between them for every state.

4.2. $\alpha + \alpha$ system

Similarly to the above, we now calculate the CLD and the scattering phase shifts of the $\alpha + \alpha$ system. The important point in the calculation of the $\alpha + \alpha$ system is the treatment of the Coulomb interaction. Because the Coulomb interaction has a long-range nature, we must include the Coulomb interaction in the asymptotic Hamiltonian H_0 .

The relative motion between two α clusters is described within the OCM as

$$\left[T_{\text{rel}} + V_{\alpha\alpha}^C(r) + V_{\alpha\alpha}^N(r) + \lambda \sum_{\text{PF}} |\phi_{\text{PF}}\rangle \langle \phi_{\text{PF}}| - E \right] \psi_{\text{rel}}^J(\mathbf{r}) = 0, \quad (4.4)$$

where $V_{\alpha\alpha}^C$ and $V_{\alpha\alpha}^N$ are the folding Coulomb and nuclear potentials obtained by assuming a $(0s_{1/2})^4$ harmonic oscillator wave function with oscillator constant $\nu_\alpha (= \frac{M\omega}{2\hbar}) = 0.2675 \text{ fm}^{-2}$ for an α cluster, respectively. When we employ the Schmid-

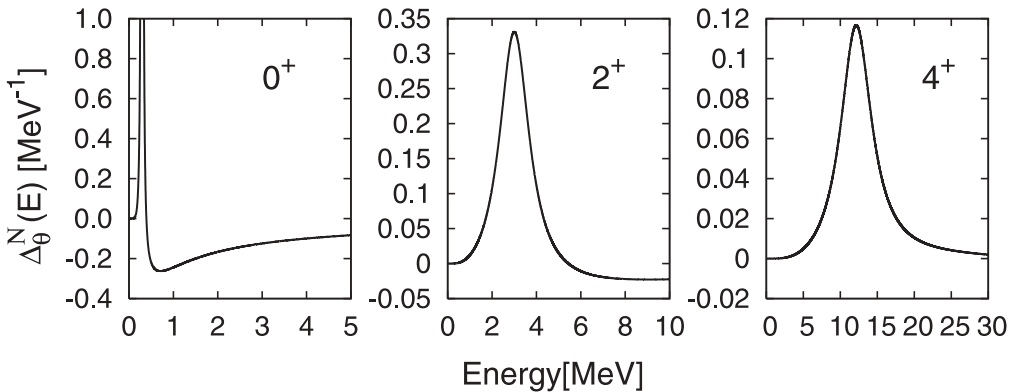


Fig. 8. Continuum level densities of the α - α system for the $J^\pi = 0^+$, 2^+ and 4^+ states.

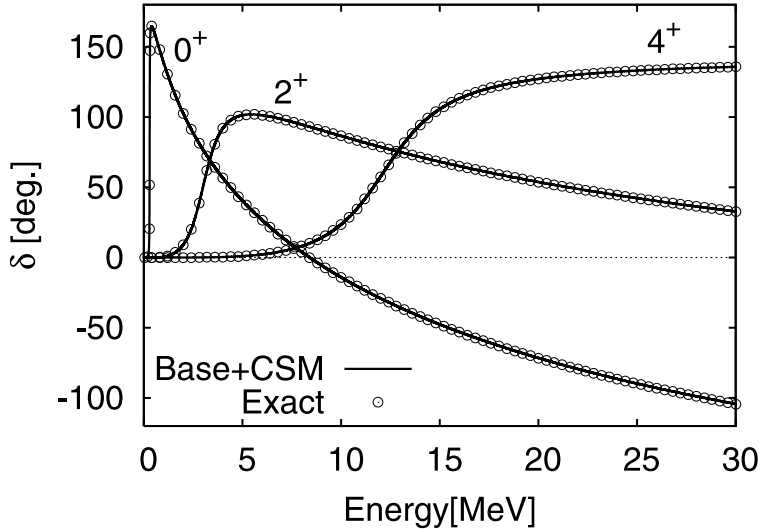


Fig. 9. Scattering phase shifts of the α - α system for the $J^\pi = 0^+$, 2^+ and 4^+ states.

Wildermuth force²⁰⁾ as the two-nucleon force, they are expressed as

$$V_{\alpha\alpha}^C(r) = \left(\frac{4e^2}{r}\right) \operatorname{erf}\left(r\sqrt{\frac{4}{3}}\nu_\alpha\right), \quad (4.5)$$

$$V_{\alpha\alpha}^N(r) = 2X_D \left[\frac{2\nu_\alpha}{2\nu_\alpha + 3\mu/2}\right]^{3/2} V_0 \exp\left[-\frac{\nu_\alpha\mu}{\nu_\alpha + 3\mu/4}r^2\right], \quad (4.6)$$

where $\operatorname{erf}(x)$ is the error function, and $X_D = 2.445$, $V_0 = -72.98$ MeV and $\mu = 0.46$ fm⁻² are the folding parameter, the strength, and the range parameter of the Schmid-Wildermuth force, respectively. The fourth term in Eq. (4.4) is the projection operator to remove the Pauli forbidden states (the $0S$, $1S$ and $0D$ states in this case) from the relative motion,¹⁸⁾ and λ is taken as 10^6 MeV as well. We solve the complex scaled Schrödinger equation Eq. (4.4) in the same way as we solved the Schrödinger equation for the simple potential and ${}^4\text{He}$ - n systems. Using the obtained eigenvalues for $J^\pi = 0^+$, 2^+ and 4^+ , we calculate the CLD. In the α - α system, however, the eigenvalues of the asymptotic Hamiltonian H_0 must be solved with the Coulomb potential:

$$H_0 = T_{\text{rel}} + \frac{4e^2}{r}. \quad (4.7)$$

The results of the CLD are shown in Fig. 8. They have a sharp peak corresponding to the resonance in each state. This result is quite similar to the results by Arai and Kruppa,⁴⁾ in which case the smoothing was performed in terms of several smoothing parameters. Better agreement is obtained for a narrower smoothing parameter.

Integrating the obtained CLD, we obtain the scattering phase shifts. The results are shown in Fig. 9. The scattering phase shifts are nearly identical to those obtained from the scattering solutions. The resonance width of the 0^+ state is very small in comparison to the resonance energy. For such a case, it is necessary to carefully

integrate the CLD to obtain accurate phase shifts. These results indicate that the present method to calculate the CLD is also very powerful even for a long-range interaction, such as the Coulomb potential.

§5. Summary and conclusion

We have shown that the level density is properly described in the CSM with a basis function method. In the expression we obtained for the level density, the extended completeness relation of the CSM plays an important role, and it divides the level density into three terms, i.e., bound states, resonances and continuum states. We investigated the approximate description of the continuum states in terms of discretized eigenstates that are obtained through diagonalization with a finite number of basis functions. Furthermore, it is not necessary to use a smoothing technique, such as the Strutinsky procedure employed by Kruppa and Arai for the singular level density arising from the discretization of continuum states. In the CSM, continuum states are expressed in terms of eigenstates of complex eigenvalues along the rotated branch cut with the angle 2θ , and the Green function of the continuum part is expressed as a sum of Lorentzian functions rather than delta functions. Therefore, no singularity appears. This result indicates that the CSM provides a very powerful method for discretizing continuum states. The discretization of a continuous function using Lorentzian functions would be understood through comparison to the wavelets²¹⁾ that have recently been developed as a powerful tool facilitating transformations between analogue and digital data in information science.

The level density smoothed in the CSM, however, has a dependence on the scaling angle θ , because a finite number of basis functions is used in the approximate description of the continuum states. We showed that the continuum level density (CLD) in the CSM, obtaining by subtracting the level density for the asymptotic Hamiltonian, is independent of the scaling angle and consistent with the exact CLD. These results indicate that we can calculate scattering phase shifts or S-matrices from the CLD obtained by solving an eigenvalue problem in the CSM with a finite number of basis functions. We found that this method is quite effective in the treatment of ${}^4\text{He}+n$ and $\alpha + \alpha$ systems without and with the Coulomb interaction, respectively, which were previously studied by Arai and Kruppa.⁴⁾

Considering the successful results of this method for simple two-body systems, it would be interesting to apply it to coupled-channel systems and three-body systems. For coupled-channel problems, the extended completeness relation providing the foundation of this method has been proven in the framework of the CSM.¹⁰⁾ Therefore, it is conjectured that the present method will be effective here too. However, the three-body problem is still open.

Acknowledgements

The authors would like to thank Dr. K. Arai for fruitful discussions. They also would like to acknowledge the members of the nuclear theory group at Hokkaido University for many discussions. This work was performed as a part of the “Research

Project for Study of Unstable Nuclei from Nuclear Cluster Aspects (SUNNCA)” sponsored by RIKEN.

References

- 1) I. Tanihata, J. of Phys. G **22** (1996), 157.
- 2) A. T. Kruppa, Phys. Lett. B **431** (1998), 237.
- 3) A. T. Kruppa and K. Arai, Phys. Rev. A **59** (1999), 3556.
- 4) K. Arai and A. T. Kruppa, Phys. Rev. C **60** (1999), 064315.
- 5) S. Shlomo, Nucl. Phys. A **539** (1992), 17.
- 6) V. M. Strutinsky, Nucl. Phys. A **95** (1967), 420.
- 7) J. Aguilar and J. M. Combes, Commun. Math. Phys. **22** (1971), 269.
E. Balslev and J. M. Combes, Commun. Math. Phys. **22** (1971), 280.
- 8) T. Myo, A. Ohnishi and K. Katō, Prog. Theor. Phys. **99** (1998), 801.
- 9) T. Berggren, Nucl. Phys. A **109** (1968), 265.
- 10) B. G. Giraud, K. Katō and A. Ohnishi, J. of Phys. A **37** (2004), 11575.
- 11) B. G. Giraud and K. Katō, Ann. of Phys. **308** (2003), 115.
- 12) R. D. Levine, *Quantum Mechanics of Molecular Rate Processes* (Clarendon Press, Oxford, 1969), p. 101.
- 13) A. Csótó, B. Gyarmati, A. T. Kruppa, K. F. Pál and N. Moiseyev, Phys. Rev. A **41** (1990), 3469.
- 14) M. Kamimura, Phys. Rev. A **38** (1988), 621.
H. Kameyama, M. Kamimura and Y. Fukushima, Phys. Rev. C **40** (1989), 974.
- 15) M. Homma, T. Myo and K. Katō, Prog. Theor. Phys. **97** (1997), 561.
- 16) S. Saito, Prog. Theor. Phys. **41** (1969), 705.
- 17) H. Kanada, T. Kaneko, S. Nagata and M. Nomoto, Prog. Theor. Phys. **61** (1979), 1327.
- 18) V. I. Kukulin, V. M. Krasnopol'sky, V. T. Voronchev and P. B. Sazonov, Nucl. Phys. A **453** (1986), 365.
- 19) S. Aoyama, S. Mukai, K. Katō and K. Ikeda, Prog. Theor. Phys. **93** (1995), 99.
- 20) E. W. Schmid and K. Wildermuth, Nucl. Phys. **26** (1961), 463.
- 21) I. Daubechies, *Ten Lectures on Wavelets* (Society for Industrial and Applied Mathematics, Philadelphia, PA, 1992).